arXiv:1111.0999v2 [cond-mat.quant-gas] 30 Aug 2012

Clock shift in a strongly interacting two-dimensional Fermi gas

Christian Langmack[1], Marcus Barth[2], Wilhelm Zwerger[2], and Eric Braaten[1]
[1] *Department of Physics, The Ohio State University, Columbus, OH 43210, USA*
[2] *Technische Universität München, Physik Department, James-Franck-Strasse, 85748 Garching, Germany*

(Dated: September 3, 2012)

We derive universal relations for the radio-frequency (rf) spectroscopy of a two-dimensional Fermi gas consisting of two spin states interacting through an S-wave scattering length. The rf transition rate has a high-frequency tail that is proportional to the contact and displays logarithmic scaling violations, decreasing asymptotically like $1/(\omega^2 \ln^2 \omega)$. Its coefficient is proportional to $\ln^2(a'_{2D}/a_{2D})$, where a_{2D} and a'_{2D} are the 2-dimensional scattering lengths associated with initial-state and final-state interactions. The clock shift is proportional to the contact and to $\ln(a'_{2D}/a_{2D})$. If $|\ln(a'_{2D}/a_{2D})| \gg 1$, the clock shift arises as a cancellation between much larger contributions proportional to $\ln^2(a'_{2D}/a_{2D})$ from bound-bound and bound-free rf transitions.

PACS numbers: 03.75.Ss, 05.30.Fk, 67.85.-d.

Spectroscopy of the internal levels of atoms is a central subject of atomic physics. The associated transition frequencies of a single atom are known with the precision of atomic clocks. In fact, atomic clocks use a hyperfine transition in cesium to keep our standard of time. In a gas, the atoms experience energy shifts due to interactions with the surrounding atoms, resulting in transition frequencies that differ from those of free atoms. Such density-dependent interaction shifts are a major source of systematic errors in atomic clocks, and are thus called *clock shifts*. Precision spectroscopy aims to avoid these shifts as far as possible, e.g. by working at extremely low densities or by using a purely spin-polarized gas of fermions in the ultracold limit where the remaining S-wave collisions are forbidden by the Pauli principle [1]. Alternatively, the atoms may be stored in an optical lattice, where both the center-of-mass motion and the interactions are completely quenched [2].

In investigations of many-body physics using ultracold gases, the clock shift is, however, a signal of interest rather than a nuisance. It can be especially interesting when the atoms are strongly interacting, i.e. their scattering length is large compared to both the range of interactions and the average interparticle distance. The interaction energy [1, 3] and the pairing gap [4] have been measured for strongly-interacting fermionic atoms near a Feshbach resonance. The generic setup for these experiments involves a gas containing atoms in just two hyperfine states $|1\rangle$ and $|2\rangle$. A radio-frequency (rf) pulse, tuned to the hyperfine splitting between $|2\rangle$ and a third, unoccupied state $|3\rangle$ will then transfer atoms from $|2\rangle$ into $|3\rangle$. If, for example, states $|1\rangle$ and $|2\rangle$ form a molecular bound state, the rf pulse has to be detuned compared to the bare hyperfine splitting by a frequency ω associated with the binding energy of the molecule. At the two-body level, effects like these can be analyzed in a straightforward manner, even in the presence of strong final-state interactions between $|1\rangle$ and $|3\rangle$ [5]. In a genuine many-body situation, however, analytic methods for calculating the rf transition rate $\Gamma(\omega)$ are not available. Exact relations for $\Gamma(\omega)$ that hold independent of density and interaction strength are therefore of considerable interest.

For strongly interacting fermions with two spin states in three dimensions (3D), a number of exact relations that connect thermodynamic variables to large-momentum and high-frequency tails of correlation functions have been derived by Tan [6, 7]. These relations all involve the contact C, which basically measures the probability for pairs of fermions in states $|1\rangle$ and $|2\rangle$ to be very close together. More precisely, the contact may be defined by the universal power-law tail

$$n_\sigma(k) \longrightarrow C/k^4, \qquad \sigma = 1, 2 \tag{1}$$

of the momentum distribution of either spin state at large momentum k. The Tan relations are universal in the sense that they apply to *any* state of the system, e.g. few-body or many-body, homogeneous or in a trapping potential, Fermi-liquid or superfluid state, provided only that the length scales associated with the temperature and number densities are large compared to the range of interactions. The origin of this universality is that the Tan relations are a consequence of operator identities, some of which follow from the operator product expansion of quantum field theory [8]. There are also universal relations governing rf spectroscopy. Specifically, the average clock shift, i.e. the first moment of $\Gamma(\omega)$, is proportional to the contact C [9] or, equivalently, to a derivative of the total energy with respect to the scattering length [10]. Moreover, the rf transition rate $\Gamma(\omega)$ has a high-frequency tail that is proportional to C and decreases like $1/\omega^n$, where the exponent n is either $\frac{5}{2}$ or $\frac{3}{2}$ depending on the strength of the final-state interactions between $|1\rangle$ and $|3\rangle$ [11–13]. Some of the universal relations have been verified experimentally, e.g. by comparing the values of C obtained from the tail of the momentum distribution in Eq. (1) and from the rf transition rate at large ω [14].

In our present work, we derive universal relations for rf spectroscopy in *two*-dimensional Fermi gases. These systems have been investigated in several recent experiments [15–17]. Beyond the motivation provided by these experiments, universal relations that constrain the rf transition rate in two dimensions (2D) are of interest also for other reasons. First, rf spectroscopy measurements can be performed within a rather short time scale. It thus allows access to not only equilibrium but also excited states of the many-body system, e.g. the polaron on the repulsive branch of a Feshbach resonance [18] or Bose gases in the regime of strong repulsion. A second reason is that a 2D gas with zero-range interactions provides an example of a non-relativistic many-body system that is scale invariant at the classical but not at the quantum level. This breaking of the scale invariance by quantum effects is an elementary example of an anomaly [19]. It implies that the coupling constant g (which will be defined explicitly below) is in fact a running coupling constant $g(\mu) = -2\pi/\ln(a_{2D}\mu)$ that changes logarithmically with the momentum scale μ, reminiscent of the coupling constant of Quantum Chromodynamics. The associated intrinsic length a_{2D} sets the scale for the two-body scattering amplitude which, at low energies, has the characteristic form [20, 21]

$$f(q) = \frac{4\pi}{\ln(1/q^2 a_{2D}^2) + i\pi}\,. \tag{2}$$

For any positive value of a_{2D}, this amplitude has a pole at $q = i/a_{2D}$, which signifies the presence of a diatomic molecule with binding energy $E_d = \hbar^2/ma_{2D}^2$ that we will call the (12)-dimer.

In experiments with ultracold atoms, the 2D gas arises from a 3D system by adding a strong transverse confining potential that restricts the atoms to the ground state in the third dimension. For harmonic trapping with angular frequency ω_z, the relation between a_{2D} and the experimentally tunable 3D scattering length a is given by $\ell/a = f_1(\ell^2/a_{2D}^2)$, where $\ell^2 = \hbar/m\omega_z$ and the function $f_1(x)$ is given in section V.A of Ref. [21].

A system consisting of fermions with the two spin states $|1\rangle$ and $|2\rangle$ can be described by a quantum field theory with the interaction Hamiltonian

$$H_{\rm int} = (g/m)\textstyle\int d^2R\, \psi_1^\dagger\psi_2^\dagger\psi_2\psi_1(\boldsymbol{R}). \tag{3}$$

Here g is the bare coupling constant, which can be identified with the running coupling constant at the momentum scale of the ultraviolet cutoff. Within this framework, universal relations for both equilibrium properties and rf spectra can be derived using the operator product expansion (OPE) [8]. In particular, the tail of the momentum distribution in Eq. (1) follows from the OPE for $\psi_\sigma^\dagger(\boldsymbol{R}+\frac{1}{2}\boldsymbol{r})\psi_\sigma(\boldsymbol{R}-\frac{1}{2}\boldsymbol{r})$. The leading contribution that is non-analytic as $\boldsymbol{r}\to 0$ comes from the operator $\psi_1^\dagger\psi_2^\dagger\psi_2\psi_1(\boldsymbol{R})$, whose coefficient exhibits a logarithmic singularity in 2D of the form $|\boldsymbol{r}|^2\log|\boldsymbol{r}|$. As a result, $n_\sigma(k)$ behaves asymptotically like C/k^4 with no logarithmic corrections, as in 3D and also in 1D [22]. The contact $C = \int d^2R\, \mathcal{C}(\boldsymbol{R})$ is an integral of the contact density

$$\mathcal{C}(\boldsymbol{R}) = g^2\langle\psi_1^\dagger\psi_2^\dagger\psi_2\psi_1(\boldsymbol{R})\rangle\,, \tag{4}$$

which is the expectation value of a local operator that annihilates and recreates a pair of fermions. The structure of these results is identical to the 3D case and, indeed, many of Tan's universal relations may be generalized to 2D [23]. Universal relations for current correlators, structure factors, and hydrodynamic correlators in 2D have also been derived using the OPE [24].

We now consider the rf spectroscopy of the 2D system consisting of fermions in states $|1\rangle$ and $|2\rangle$. Beyond the interaction described by a_{2D}, we also include final-state interactions between $|1\rangle$ and $|3\rangle$ with 2D scattering length a'_{2D}. We will refer to the diatomic molecule consisting of $|1\rangle$ and $|3\rangle$, which has binding energy $E'_d = \hbar^2/m{a'_{2D}}^2$, as the (13)-dimer. The transfer rate $\Gamma(\omega)$ between $|2\rangle$ and $|3\rangle$ can be expressed in terms of the imaginary part of a time-ordered correlation function:

$$\Gamma(\omega) = \Omega^2 \textstyle\int d^2R\; \mathrm{Im}\left(i\,\langle\mathcal{O}_{\rm rf}(\omega+i\epsilon,\boldsymbol{R})\rangle\right), \tag{5}$$

where Ω is the Rabi frequency of the rf transition and $\mathcal{O}_{\rm rf}(\omega,\boldsymbol{R})$ is an operator that depends on a complex variable ω:

$$\begin{aligned}\mathcal{O}_{\rm rf}(\omega,\boldsymbol{R}) = {}&\textstyle\int dt\; e^{i\omega t}\int d^2r\\ &\times\mathcal{T}\psi_2^\dagger\psi_3\left(\boldsymbol{R}+\tfrac{1}{2}\boldsymbol{r},t\right)\psi_3^\dagger\psi_2\left(\boldsymbol{R}-\tfrac{1}{2}\boldsymbol{r},0\right).\end{aligned} \tag{6}$$

(The time-ordering symbol $\mathcal{T}$ acts on all operators to the right.) The bilocal operator can be expanded in terms of local operators by using the OPE:

$$\mathcal{O}_{\rm rf}(\omega,\boldsymbol{R}) = \textstyle\sum_n C_n(\omega)\mathcal{O}_n(\boldsymbol{R}). \tag{7}$$

Local operators can be assigned scaling dimensions. The quantum fields ψ_σ have dimension 1. The gradient ∇ and the time derivative $\partial/\partial t$ increase the dimension by 1 and 2, respectively. At large frequency ω, higher dimension operators in the OPE have Wilson coefficients $C_n(\omega)$ that decrease with higher powers of ω. The Wilson coefficients $C_n(\omega)$ in Eq. (7) can be calculated by matching Green functions of the bilocal rf operator on the left side of the OPE with Green functions of the local operators on the right side. For operators of dimensions 2 and 4, it is sufficient to match the Green functions in the 1-atom and 2-atom sectors. Our final result for the expectation value of $\mathcal{O}_{\rm rf}(\omega,\boldsymbol{R})$ at large complex ω, including all operators with dimensions up to 4, is

$$\begin{aligned}\langle\mathcal{O}_{\rm rf}(\omega,\boldsymbol{R})\rangle\longrightarrow{}& \frac{i}{\omega}n_2(\boldsymbol{R}) + \frac{i\,\nabla^2 n_2(\boldsymbol{R}) + 4m\nabla\cdot\boldsymbol{J}_2(\boldsymbol{R})}{8m\omega^2}\\ &+\frac{i\ln(a'_{2D}/a_{2D})\ln(a_{2D}\sqrt{-m\omega}\,)}{2\pi m\omega^2\ln(a'_{2D}\sqrt{-m\omega}\,)}\mathcal{C}(\boldsymbol{R}),\end{aligned} \tag{8}$$

where n_2 and $\boldsymbol{J}_2$ are the number density and current density for $|2\rangle$. If the system is in a steady state, $\nabla \cdot \boldsymbol{J}_2$ vanishes because of current conservation. The integral of $\nabla^2 n_2$ vanishes by the divergence theorem. The terms shown explicitly in Eq. (8) are not affected by final-state interactions between $|2\rangle$ and $|3\rangle$, which first enter into the coefficients of dimension-6 operators.

We can derive various universal relations from the OPE in Eq. (8). The tail of the rf transition rate at large positive frequencies ω can be obtained by extrapolating Eq. (8) to the real axis, taking the imaginary part, and then inserting it into Eq. (5):

$$\Gamma(\omega) \longrightarrow \frac{\ln^2(E_d'/E_d)\Omega^2 C}{4m\omega^2\left[\ln^2(\omega/E_d') + \pi^2\right]}. \tag{9}$$

Higher dimension operators in the OPE give contributions to the high-frequency tail that decrease faster than ω^{-3}. These contributions are suppressed by a positive power of an energy scale of the many-body system divided by ω. The relevant energy scales of the many-body system include E_d, the thermal energy $k_B T$, and the two Fermi energies $4\pi^2 n_1/m$ and $4\pi^2 n_2/m$. The factor $\ln^2(E_d'/E_d)$ in Eq. (9) can be interpreted as $16\pi^2/g^2(1/a_{2D}')$, where $g(1/a_{2D}')$ is the running coupling constant at the momentum scale $1/a_{2D}'$. If $a_{2D}' = a_{2D}$, the high-frequency tail in Eq. (9) vanishes identically. In this case, $\Gamma(\omega)$ just consists of an unshifted peak $\pi\Omega^2 N_2 \delta(\omega)$, because the rf pulse merely rotates $|2\rangle$ and $|3\rangle$ in spin space [10]. The nontrivial dependence on ω in Eq. (9) is a consequence of the anomalous scale invariance. If $|\ln(\omega/E_d')| \ll \pi$, the high-frequency tail in Eq. (9) has the simple scaling behavior $\Gamma(\omega) \sim 1/\omega^2$. However at much larger or much smaller frequencies, there are logarithmic scaling violations and the asymptotic behavior is $\Gamma(\omega) \sim (\omega^2 \ln^2 \omega)^{-1}$. Simple scaling behavior also arises in the limit of negligible final-state interactions in which $\ln(E_d'/\omega) \to \infty$. In this limit, the high-frequency tail in Eq. (9) reduces to $\Omega^2 C/4m\omega^2$. This relation has been used in recent experiments with ^{40}K atoms to extract the contact density in the normal state of the 2D Fermi gas [25]. The contact density and its dependence on a_{2D} is close to that obtained from variational Monte Carlo calculations at $T = 0$ [26].

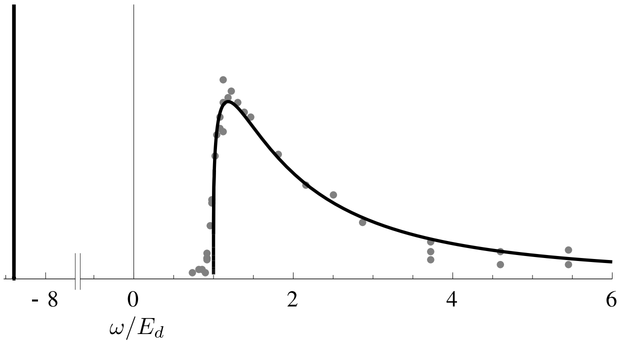

FIG. 1. Rf transition rate for the (12)-dimer as a function of ω/E_d for the case $E_d' = 9.4E_d$. There is a delta function at $\omega = -(E_d' - E_d)$ from the bound-bound transition. The threshold for bound-free transitions is at $\omega = E_d$. The grey dots in the bound-free region are data from Zwierlein and collaborators [27], normalized by a least-squares fit to the theory curve.

Sum rules can be derived by expressing weighted integrals of $\Gamma(\omega)$ as contour integrals in the complex-ω plane:

$$\int_{-\infty}^{+\infty} d\omega f(\omega)\Gamma(\omega) = \frac{\Omega^2}{2}\int d^2R \oint d\omega f(\omega)\langle \mathcal{O}_{\rm rf}(\omega, \boldsymbol{R})\rangle, \tag{10}$$

where the ω contour runs from $+\infty$ to $-\infty$ just below the real axis and then from $-\infty$ to $+\infty$ just above the axis. If the contour is deformed into a circle of infinite radius, the OPE in Eq. (8) will be exact everywhere on the contour. Choosing $f(\omega) = 1$ and $f(\omega) = \omega$, we obtain

$$\int_{-\infty}^{+\infty} d\omega\, \Gamma(\omega) = \pi\Omega^2 N_2, \tag{11a}$$

$$\int_{-\infty}^{+\infty} d\omega\, \omega\Gamma(\omega) = \frac{\ln(a_{2D}'/a_{2D})\Omega^2 C}{2m}. \tag{11b}$$

These sum rules are exact: they receive no contributions from higher dimension operators in the OPE. The first sum rule guarantees that interactions do not change the integrated rf signal. The second sum rule determines the clock shift $\langle\omega\rangle$, which is defined as the ratio of the integrals in Eqs. (11):

$$\langle\omega\rangle = -\frac{\ln(E_d'/E_d)\, C}{4\pi m N_2}. \tag{12}$$

Note that both the clock shift and the tail of the rf transition rate in Eq. (9) are unaffected by final-state interactions between $|2\rangle$ and $|3\rangle$.

The universal relations in Eqs. (9) and (11) can be illustrated by considering rf spectroscopy on the two-body system consisting of a single (12)-dimer with binding energy E_d. The rf transition rate is

$$\begin{aligned}\Gamma(\omega) = {}& \frac{\pi\Omega^2 E_d' E_d \ln^2(E_d'/E_d)}{(E_d' - E_d)^2}\, \delta(\omega - E_d + E_d') \\ &+ \frac{\pi\Omega^2 E_d \ln^2(E_d'/E_d)}{\omega^2[\ln^2((\omega - E_d)/E_d') + \pi^2]}\, \theta(\omega - E_d).\end{aligned} \tag{13}$$

By evaluating the integrals in Eqs. (11), we verify that the sum rules are satisfied exactly with $N_2 = 1$ and $C = 4\pi m E_d$, the contact for the (12)-dimer obtained from the adiabatic universal relation $dE_d/da_{2D} = -C/(2\pi m a_{2D})$ [23]. The universal relation for the tail in Eq. (9) holds for $|\omega| \gg E_d$. The clock shift for the (12)-dimer has a negative contribution proportional to $\ln^2(E_d'/E_d)$ from bound-bound transitions. If $|\ln(E_d'/E_d)| \gg 1$, there is a large canceling contribution from bound-free transitions, such that the total clock shift agrees with Eq. (12). Near the threshold, the bound-free transition rate has the behavior $1/\ln^2((\omega - E_d)/E'_d)$. This follows from the inverse-logarithmic behavior of the two-body scattering amplitude for $|1\rangle$ and $|3\rangle$ analogous to Eq. (2). Recent experiments using ^{6}Li atoms in 2D [17] are in good agreement with the bound-free transition rate in Eq. (13) for a single (12)-dimer in the presence of final-state interactions. The data in Fig. 1 [27] were measured near the 3D Feshbach resonance for $|1\rangle$ and $|2\rangle$ at a magnetic field of 690.7 G and a lattice depth to recoil energy ratio of 18.6(7), and they extend out to higher ω than in Ref. [17]. The ratio E'_d/E_d is around 9.4 and E_d is about a factor 6 larger than the Fermi energy [27]. This places the system in the BEC limit of the many-body problem where the two-body result in Eq. (13) applies.

We now consider the many-body system in the limit in which E'_d is much greater than E_d and the other relevant energy scales. The bound-bound and free-bound region is then well separated from the free-free and free-bound region of the rf spectrum. There could be additional structure in the region of ω between $-(E'_d - E_d)$ and 0 associated with clusters of three or more atoms. However, if this region is featureless, it is useful to define a clock shift for the rf transition rate restricted to a range of frequencies $-\omega_0 < \omega < \omega_0$ that excludes the bound-bound peak. We choose ω_0 and $E'_d - \omega_0$ to be much greater than the energy scales of the system. This clock shift is given by a ratio of integrals analogous to those in Eq. (11). They can be expressed as contour integrals analogous to those in Eq.(10), except that the contour runs from $+\omega_0$ to $-\omega_0$ just below the real axis and then back to $+\omega_0$ just above the axis. If the contour is deformed into a circle of radius ω_0, we can apply the OPE in Eq. (8) and obtain the sum rules

$$\int_{-\omega_0}^{+\omega_0} d\omega\, \Gamma(\omega) = \pi\Omega^2 N_2 - [\mathrm{Im}\,\mathrm{Ei}(-L_0 + i\pi)] \times \left(\ln\frac{a'_{2D}}{a_{2D}}\right) \frac{\Omega^2 C}{\pi m E'_d} + \ldots, \tag{14a}$$

$$\int_{-\omega_0}^{+\omega_0} d\omega\, \omega\Gamma(\omega) = \left(\ln\frac{a'_{2D}}{a_{2D}} - \frac{2}{\pi}\ln^2\frac{a'_{2D}}{a_{2D}} \arctan\frac{\pi}{L_0}\right)\frac{\Omega^2 C}{2m} + \ldots, \tag{14b}$$

where $\mathrm{Ei}(x)$ is the exponential integral function and $L_0 = \ln(\omega_0/E'_d)$. One advantage of finite-frequency sum rules such as those in Eqs. (14) is that they can be evaluated using measured rf spectra without extrapolations to larger frequencies. As indicated by "$+\ldots$" in Eqs. (14), these sum rules are not exact. They receive contributions from higher dimensional operators in the OPE that are suppressed by powers of an energy scale of the system divided by ω_0 or E'_d. For example, the higher dimension contribution in Eq. (14a) is suppressed by a factor of $C/mE'_d N_2$. The corrections that are suppressed by inverse powers of ω_0 can be minimized by choosing ω_0 as large as possible while still avoiding contributions from the bound-bound peak. Neglecting the contributions from higher dimension operators, the clock shift obtained from Eqs. (14) reduces to

$$\langle\omega\rangle = \left(\frac{1}{\pi}\ln^2\frac{E'_d}{E_d}\arctan\frac{\pi}{|L_0|} - \ln\frac{E'_d}{E_d}\right)\frac{C}{4\pi m N_2}\,. \tag{15}$$

If $|\ln(E'_d/E_d)| \gg 1$, this clock shift is much larger than that in Eq. (12). The clock shift in Eq. (15), which excludes the contribution from bound-bound transitions, is the one that is more relevant to the limit of weak final-state interactions. The factor $\ln^2(E'_d/E_d)$ diverges in the limit $a'_{2D} \to 0$, indicating that the clock shift in this case is quadratically logarithmically sensitive to the range of interactions.

In summary, we have presented universal relations for the rf spectroscopy of strongly interacting fermions in a 2D Fermi gas. They are of direct relevance to current experiments with ultracold atoms, providing rigorous connections between rf spectrocopy, thermodynamics, and various correlation functions. They reveal aspects of these many-body systems that are directly related to the breaking of scale invariance in 2D and will hopefully provide inspiration for further investigations of these unusual systems.

This research was supported in part by a joint grant from the ARO and the AFOSR and by the DFG. We acknowledge valuable discussions with M. Köhl, R. Schmidt, A. Sommer, and M. Zwierlein and we thank the latter two for making their data available.

[1] S. Gupta et al., Science **300**, 1723 (2003).
[2] M. Swallows et al., Science **331**, 1043 (2011).
[3] C. A. Regal and D. S. Jin, Phys. Rev. Lett. **90**, 230404 (2003).
[4] C. Chin et al., Science **305**, 1128 (2004).
[5] C. Chin and P. S. Julienne, Phys. Rev. A **71**, 012713 (2005).
[6] S. Tan, Ann. Phys. (N.Y.) **323**, 2952 (2008); **323**, 2971 (2008); **323**, 2987 (2008).
[7] E. Braaten, in *The BCS-BEC Crossover and the Unitary Fermi Gas*, edited by W. Zwerger (Springer-Verlag, 2012).
[8] E. Braaten and L. Platter, Phys. Rev. Lett. **100**, 205301 (2008).
[9] M. Punk and W. Zwerger, Phys. Rev. Lett. **99**, 170404 (2007).
[10] G. Baym, C.J. Pethick, Z. Yu, and M.W. Zwierlein, Phys. Rev. Lett. **99**, 190407 (2007).
[11] R. Haussmann, M. Punk, and W. Zwerger, Phys. Rev. A **80**, 063612 (2009).
[12] W. Schneider and M. Randeria, Phys. Rev. A **81**, 021601 (2010).
[13] E. Braaten, D. Kang, and L. Platter, Phys. Rev. Lett. **104**, 223004 (2010).

[14] J.T. Stewart, J.P. Gaebler, T.E. Drake, and D.S. Jin, Phys. Rev. Lett. **104**, 235301 (2010).

[15] B. Fröhlich et al., Phys. Rev. Lett. **106**, 105301 (2011).

[16] M. Feld et al., Nature (London) **480**, 75 (2011).

[17] A. Sommer et al., Phys Rev. Lett. **108**, 045302 (2012).

[18] R. Schmidt, T. Enss, V. Pietilä, and E. Demler, Phys. Rev. A **85**, 021602(R) (2012).

[19] B. Holstein, Am. J. Phys. **61**, 142 (1993).

[20] D.S. Petrov and G.V. Shlyapnikov, Phys. Rev. A **64** 012706 (2001).

[21] I. Bloch, J. Dalibard, and W. Zwerger, Rev. Mod. Phys. **80**, 885 (2008).

[22] M. Barth and W. Zwerger, Ann. Phys. **326**, 2544 (2011).

[23] F. Werner and Y. Castin, arXiv:1001.0774.

[24] J. Hofmann, Phys. Rev. A. **84**, 043603 (2011).

[25] B. Fröhlich, Ph.D. thesis, University of Cambridge, July 2011.

[26] G. Bertaina and S. Giorgini, Phys. Rev. Lett. **106**, 110403 (2011).

[27] A. Sommer and M. Zwierlein, private communication.